Molecular Microbiology (2012) 85(4), 734–746 ■
doi:10.1111/j.1365-2958.2012.08135.x
First published online 16 July 2012

Activity of the tetrapyrrole regulator CrtJ is controlled by oxidation of a redox active cysteine located in the DNA binding domain

Zhuo Cheng,[1] Jiang Wu,[1] Aaron Setterdahl,[1] Khalilah Reddie,[3] Kate Carroll,[4] Loubna A. Hammad,[2] Jonathan A. Karty[2] and Carl E. Bauer[1]*

Departments of [1]Molecular and Cellular Biochemistry and [2]Chemistry, Indiana University, Bloomington, IN 47405, USA.

[3]Life Sciences Institute, University of Michigan, Ann Arbor, MI 48109, USA.

[4]Department of Chemistry, The Scripps Research Institute, Florida Campus, Jupiter, FL 33458, USA.

Summary

CrtJ from *Rhodobacter capsulatus* is a regulator of genes involved in the biosynthesis of haem, bacteriochlorophyll, carotenoids as well as structural proteins of the light harvesting-II complex. Fluorescence anisotropy-based DNA-binding analysis demonstrates that oxidized CrtJ exhibits ~ 20-fold increase in binding affinity over that of reduced CrtJ. Liquid chromatography electrospray tandem ionization mass spectrometric analysis using DAz-2, a sulfenic acid (–SOH)-specific probe, demonstrates that exposure of CrtJ to oxygen or to hydrogen peroxide leads to significant accumulation of a sulfenic acid derivative of Cys420 which is located in the helix–turn–helix (HTH) motif. *In vivo* labelling with 4-(3-azidopropyl) cyclohexane-1,3-dione (DAz-2) shows that Cys420 also forms a sulfenic acid modification *in vivo* when cells are exposed to oxygen. Moreover, a Cys420 to Ala mutation leads to a ~ 60-fold reduction of DNA binding activity while a Cys to Ser substitution at position 420 that mimics a cysteine sulfenic acid results in a ~ 4-fold increase in DNA binding activity. These results provide the first example where sulfenic acid oxidation of a cysteine in a HTH-motif leads to differential effects on gene expression.

Accepted 12 June, 2012. *For correspondence. E-mail bauer@indiana.edu; Tel. (+1) 812 855 6595; Fax (+1) 812 856 5710.

Introduction

The α-proteobacterium *Rhodobacter capsulatus* is a model organism for studying how oxygen affects the physiology of bacteria (Imhoff *et al*., 1984). As is the case of all photosynthetic organisms, this species must tightly regulate biosynthesis of bacteriochlorophyll and carotenoids with apoproteins of the photosystem (Cohen-Bazire *et al*., 1957; Bauer, 2001). In addition, there is co-ordination of haem and cytochrome apoprotein biosynthesis with components of the photosystem (Bauer and Bird, 1996). One of the main regulators responsible for this co-ordination is the redox responding repressor CrtJ (Penfold and Pemberton, 1991; Ponnampalam *et al*., 1995).

Previous studies have demonstrated that CrtJ binds promoters containing two conserved palindromes ($TGTN_{12}ACA$) with binding enhanced by the presence of oxygen (Ponnampalam and Bauer, 1997; Elsen *et al*., 1998). It was proposed that redox-regulated binding is dependent on the formation of an intramolecular disulfide bond between cysteine residues Cys249 and Cys420, although direct evidence for formation of this bond has not been presented (Masuda *et al*., 2002). A sequence alignment of various CrtJ homologues reveals that only Cys420 located in the HTH DNA recognition motif, is conserved (Fig. S1) (Kovacs *et al*., 2005). Additional studies have shown that a Cys to Ala mutation at Cys420 elevated aerobic expression of photosynthesis genes to the same level as a *crtJ* deletion strain (Masuda *et al*., 2002). This is contrasted by an Ala mutation at Cys249 that only partially derepressed aerobic photosystem expression (Masuda *et al*., 2002). These observations suggest that alterations of the redox state of Cys420, beyond disulfide bond formation, is a major contributor to redox regulation of CrtJ DNA binding activity.

In several respects, the regulation of CrtJ resembles OxyR from *Escherichia coli* that controls synthesis of oxidative defence proteins in response to hydrogen peroxide. Initial experiments demonstrated that exposure of OxyR to hydrogen peroxide resulted in the formation of a disulfide bond that affected the DNA binding activity (Zheng *et al*., 1998). However, this model became more complex when it was shown that a mutation in one of the disulfide bond

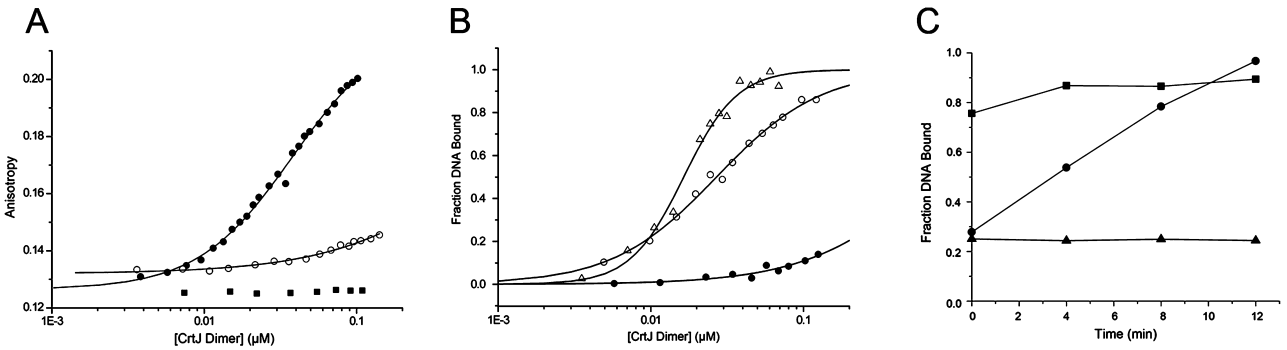

Fig. 1. Redox-dependent DNA binding by CrtJ. Representative fluorescence anisotropy-based DNA binding isotherms for (A) air oxidized CrtJ binding to the *bchC* promoter probe in the presence of 5 mM DTT (open circles) and in the absence of DTT (solid circles), or CrtJ binding to a fluorescein labelled non-specific DNA probe (solid squares).
B. Reduced CrtJ binding to the *bchC* promoter probe in a degassed basic binding buffer (solid circles), or in the degassed basic binding buffer containing 10 μM H_2O_2 (open circles) or in the degassed basic binding buffer bubbled with O_2 for 10 min (open triangles). The O_2 saturated buffer contains ~ 250 μM O_2 at 25°C. The reduced and H_2O_2 binding assays were conducted in a sealed cuvette filled with argon gas while the O_2 binding assay was conducted in an unsealed cuvette. The stock concentration of CrtJ used in the anisotropy titration is ~ 10 μM. Continuous line through each binding isotherm represents a non-linear regression analysis fitted to the Hill equation.
C. DNA binding activity of CrtJ was monitored by fluorescence anisotropy. 100 nM reduced CrtJ was first added into DNA probe in a sealed cuvette and then the cuvette was unsealed and O_2 was bubbled to the binding buffer for 1 min (Fig. 1C solid circles). 100 nM reduced CrtJ was also added into the DNA probe in a sealed cuvette without introduction of O_2 as a reduced control (Fig. 1C solid triangle). Conversely, 100 nM of oxidized CrtJ was added into the DNA probe in an unsealed cuvette as an aerobic control (Fig. 1C solid square). Fluorescence anisotropy was measured every 4 min with time 0 denoting the point at which O_2 introduced to the binding reaction. The saturated anisotropy value was obtained by fitting the data for oxidized CrtJ under aerobic condition.

forming cysteines (Cys199) exhibited more severe phenotype than did a mutation in the other disulfide bond-forming cysteine (Cys208) (Kullik *et al*., 1995). Additional experiments demonstrated that exposure of OxyR to hydrogen peroxide led to the formation of a Cys199–Cys208 disulfide bond as well as the formation of –SOH, –SNO, and –SSG oxidative modifications of the thiol on Cys199. Different oxidized forms of Cys199 exhibited different DNA binding activity indicating that OxyR is not regulated by a simple 'on and off' switch and is instead regulated more like a rheostat where binding activity is differentially regulated by different types of oxidation events at Cys199 (Kim *et al*., 2002). Beyond studies with OxyR, it has also been determined that cysteine sulfenic acids (Cys–SOH) play important roles in the regulation of several transcription factors including OhrR and Gpx3/Yap1 in yeast (Fuangthong and Helmann, 2002; Paulsen and Carroll, 2009).

The recent development of chemical agents that specifically react with oxidized derivatives of cysteine, such as 4-(3-azidopropyl)cyclohexane-1,3-dione (DAz-2), that forms an adduct with sulfenic acid derivatives of cysteine (–SOH), has shown that cells contain numerous proteins that can form stable sulfenic acid oxidized cysteines (Leonard *et al*., 2009). In most cases, the identities of proteins with redox active cysteine, as well as what effects the different oxidative modifications of a cysteine thiol have on activity, are yet to be determined. In this study, we have utilized DAz-2 to show that CrtJ forms a stable sulfenic acid modification *in vitro* and *in vivo* at Cys420 which is located in the HTH DNA-binding motif. A Cys to Ser mutation at position 420 that mimics sulfenic acid also has constitutive DNA binding activity both *in vivo* and *in vitro*. These observations indicate that exposure of CrtJ to oxygen or H_2O_2 leads to the formation of several stable oxidative modifications of Cys420 that stimulate DNA binding activity.

Results

CrtJ exhibits redox-dependent DNA binding activity

We quantified what effect redox changes have on the activity of CrtJ by undertaking fluorescence anisotropy measurements of DNA binding under oxidizing and reducing conditions. For this analysis, purified CrtJ was titrated into a fluorescein labelled double strand 54 bp segment of the *bchC* promoter that contained two CrtJ recognition palindromes. The binding affinity of oxidized CrtJ under reducing conditions [5 mM dithiothreitol (DTT)] was a rather modest EC_{50} = 822 ± 151 nM which is contrasted to a ~ 20-fold lower EC_{50} = 43 ± 20 nM observed under air oxidizing condition (Fig. 1A and Table 1). We also observed that exposure of reduced CrtJ (~ 10 μM) to an equimolar concentration of hydrogen peroxide, or buffer bubbled with O_2, can also effectively activate the DNA binding activity of CrtJ, with an EC_{50} of 34 ± 3 nM and 35 ± 6 nM respectively (Fig. 1B and Table 1).

Rapid activation of CrtJ by exposure to O_2 can also be observed by shifting a DNA binding assay containing reduced CrtJ from anaerobic to aerobic condition. As shown in Fig. 1C, when 100 nM of reduced CrtJ is anaerobically added into a sealed cuvette containing

Table 1. Summary of WT CrtJ and CrtJ mutant DNA binding affinities under different redox conditions.

CrtJ	Buffer condition[a]	EC_{50}[b] (nM)
WT	Aerobic	43 ± 20
	5 mM DTT	822 ± 151[c]
	10 μM H_2O_2	34 ± 3
	Bubbled O_2	35 ± 6
	20 mM $NaAsO_2$	85 ± 33
C249A	Aerobic	45 ± 25
	5 mM DTT	552 ± 115[c]
C420A	Aerobic	2498 ± 1176[c]
C420S	Aerobic	11 ± 7
	5 mM DTT	14 ± 7

a. Basic CrtJ-DNA binding buffer (50 mM Tris-HCl at pH 8.0, 300 mM NaCl, 2 mM $MgCl_2$, and 6% glycerol) in the presence of air, 25°C.
b. The resulting data were fitted to a cooperative binding model, using Hill equation (See *Experimental procedures* Eq. 1). EC_{50} values are averaged values of a minimum three independent fluorescence anisotropy titrations of three different protein preps.
c. Since WT CrtJ and C249A CrtJ mutant DNA binding under 5 mM DTT buffer condition and C420A under aerobic buffer condition do not reach saturation under, the maximum anisotropy value was fixed at the same value as that obtained for WT CrtJ under basic DNA-CrtJ binding buffer.

argon in the headspace there is no significant binding to the DNA probe during a 12 min incubation period (Fig. 1C solid triangles). This is contrasted by a rapid increase in binding to the DNA probe when 100 nM reduced CrtJ is first added to a sealed cuvette containing argon and then unsealed and bubbled with air for 1 min (Fig. 1C solid circles). After air exposure there is a rapid increase in DNA binding during a 12 min incubation period that saturates to the same level of binding (~ 100% probe binding) as is observed an air oxidized CrtJ control assayed in an aerobic buffer (Fig. 1C solid square). These results confirm less quantitative studies (Ponnampalam and Bauer, 1997), which indicated that CrtJ binds target DNA with a higher affinity under oxidizing conditions than under reducing conditions and that the simple exposure of CrtJ to O_2 causes rapid oxidation.

Quantification of free and modified thiols in vitro

We quantified the amount of free thiols by titrating *p*-chloromercuribenzoate (*p*-CMB) into buffer containing CrtJ. A linear increase in the 250 nm region of the spectrum occurs by mercaptide formation through reaction of *p*-CMB with free thiol groups (Boyer, 1954). With this analysis, we determined that air oxidized CrtJ contains ~ 1.5 free thiols per monomer (Fig. 2A). Oxidation of CrtJ with H_2O_2 resulted in ~ 1 free thiol per monomer which would occur if Cys249 and Cys420 were both in an oxidized state leaving only Cys22 as a free thiol (Fig. 2A). We also assayed the amount of free thiols in air oxidized CrtJ after exposing to sodium arsenite that can specifically reduce sulfenic acid (–SOH) to a free thiol (Torchinsky, 1981). By determining the free thiol content before and after sodium arsenite treatment, we can obtain a measurement of the amount of sulfenic acids present in the air oxidized preparation. This result (Fig. 2A) shows that air oxidized CrtJ has ~ 0.7 sulfenic acid per monomer. Similarly, the difference in free thiol content between the DTT (~ 2.8 free thiol per monomer) and sodium arsenite (~ 2.4 free thiol per monomer) treated samples indicate that air oxidized CrtJ that has ~ 0.4 cysteine residues in the disulfide bond form per monomer. Finally, there are small amounts of thiols (~ 0.2 per monomer) that are not reduced by DTT which likely constitute cysteine residues that form higher oxidative derivatives, sulfinic acid ($–SO_2H$) or sulfonic acid ($–SO_3H$) that are resistant to reduction by DTT.

Specific detection of sulfenic acid (–SOH) *in vitro* was also confirmed by reacting CrtJ with the electrophile 7-chloro-4-nitrobenz-2-oxa-1,3-diazole (NBD-Cl)

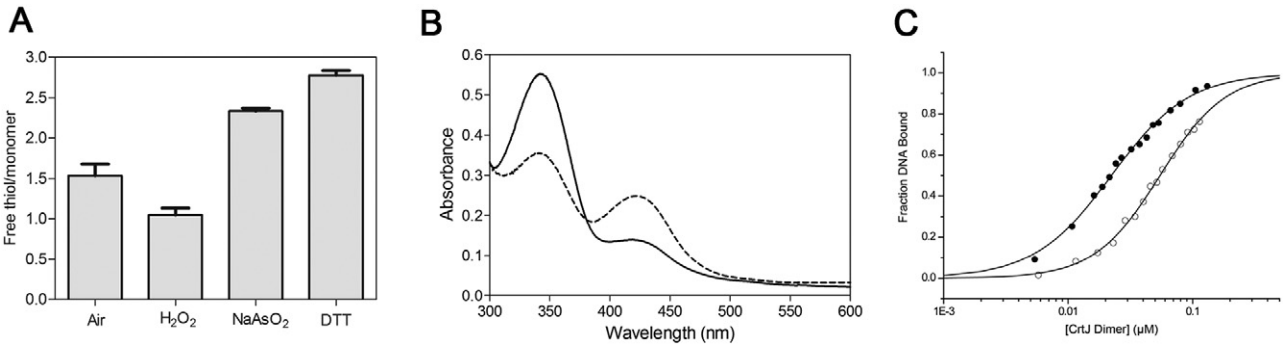

Fig. 2. Characterization of free and modified thiols of CrtJ *in vitro*.
A. Quantification of free thiol in air-oxidized CrtJ by treatment with *p*-CMB. ~ 20 μM CrtJ treated with 1 equivalent of H_2O_2, 20 mM sodium arsenite, or DDT prior to treatment with *p*-CMB.
B. Spectroscopic characteristics of NBD-modified CrtJ. Reaction of NBD with air oxidized CrtJ (solid line) and DTT reduced CrtJ (dashed line).
C. Representative normalized fluorescence anisotropy-based *bchC* promoter probe DNA binding isotherms for air oxidized WT CrtJ in the presence of 20 mM sodium arsenate (open circles) and in the absence of sodium arsenate (solid circles). Continuous line through each binding isotherm represents a non-linear regression analysis fit to Hill equation.

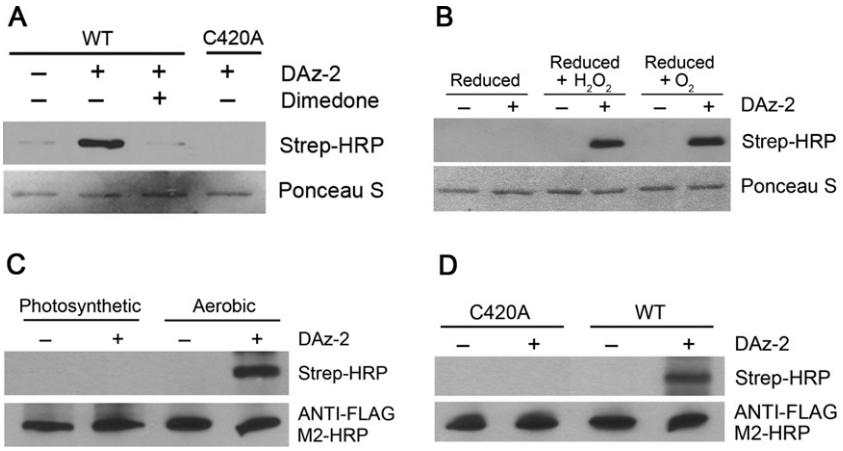

Fig. 3. DAz-2 labels sulfenic acid modified CrtJ *in vitro* and *in vivo*.
A. Visualization of recombinant CrtJ–SOH group *in vitro*. No DAz-2 and No dimedone treatment is a negative DMSO solvent control. –SOH modification of WT CrtJ is labelled upon treatment with only DAz-2, which can be competitively inhibited by first treating WT CrtJ with dimedone prior to DAz-2 treatment. Specificity of labelling at Cys420 is observed by the absence of DAz-2 labelling with the CrtJ C420A mutant.
B. Redox sensitivity of the CrtJ–SOH group *in vitro*. The treatments for WT CrtJ are shown above the blot image with reduced WT CrtJ either exposed to DAz-2 directly, or first treated with 1 equivalent H_2O_2 at RT for 30 min in an anaerobic hood prior to addition of DAz-2 or exposed to air for 30 min at RT outside the hood and then treated with DAz-2.
C. *In vivo* labelling of CrtJ–SOH group in WT CrtJ–FLAG under different growth conditions. The growth conditions (photosynthetic-lack of O_2, aerobic-in the presence O_2) are shown above the blot image.
D. *In vivo* labelling of CrtJ–SOH group at Cys420 in WT CrtJ–FLAG strain grown under aerobic condition. Specificity of labelling is shown by the absence of labelling of the mutant C420A–FLAG strain.
In panels A and B equal protein concentration is shown by staining with Ponceau S. In panels C and D the protein concentration was assayed with a parallel gel electrophoresis that utilized ANTI-FLAG M2-HRP antibody for Western blot analyses.

(Torchinsky, 1981). NBD-Cl reacts with both free thiol and sulfenic acid resulting in two different end-products that exhibit absorption at 420 nm and 347 nm respectively (Birkett *et al.*, 1970). Spectral analysis of air oxidized CrtJ reacted with NBD-Cl shows clear absorbance peaks at 347 nm indicating the presence of sulfenic acid (Fig. 2B, solid line). Reduction of air oxidized CrtJ with DTT, followed by treatment with NBD-Cl, shows an increase in the 420 nm free thiol peak and a decrease in the 347 nm sulfenic acid peak (Fig. 2B, dashed line), which indicated that sulfenic acid was reduced to a free thiol when treated with DTT.

We also tested whether the presence of a sulfenic acid group can affect the DNA binding activity of CrtJ. For this analysis, we undertook fluorescence anisotropy measurements as described above with air oxidized CrtJ in the absence or presence of 20 mM sodium arsenite. As shown in Fig. 2C, and quantified in Table 1, specific reduction of sulfenic acid to a free thiol by sodium arsenite results in a ~ 2-fold decrease in DNA binding affinity of air oxidized CrtJ. This clearly indicates that the DNA binding affinity of air oxidized CrtJ is stimulated by the presence of a sulfenic acid derivative of Cys. Interestingly, the ~ 2-fold reduction in activity by addition of sodium arsenite pales in comparison with a ~ 20-fold reduction in DNA binding activity observed by addition of DTT (Table 1) that reduces disulfides as well as sulfenic acid. This indicates either that a substantial fraction of air oxidized CrtJ is in the disulfide bond form which is not supported by our quantification of free thiols experiments (Fig. 2A) or more likely that a mixed population of sulfenic acid and disulfide bonded forms of CrtJ exist that have a similar binding affinity. If the latter is occurring then treatment with sodium arsenite would only have minor effect on the DNA binding activity of CrtJ as the remaining disulfide bonded protein would still effectively bind to the probe.

CrtJ Cys420 Forms an –SOH group in vitro *and* in vivo

We detected sulfenic acid modified CrtJ *in vitro* and *in vivo* utilizing DAz-2, a sulfenic acid-specific probe. DAz-2 is cell permeable and contains an azide handle that can be selectively linked to a biotin group via the Staudinger ligation so that the DAz-2 labelled proteins can be detected by Western blot using streptavidin-HRP (Leonard *et al.*, 2009). We observed that aerobically oxidized CrtJ is readily labelled *in vitro* by DAz-2, confirming the presence of sulfenic acid (Fig. 3A). This result is contrasted by analysis of a Cys to Ala substitution mutation of CrtJ at position 420 (CrtJ C420A) that exhibits no *in vitro* labelling by DAz-2 (Fig. 3A).

Redox reactivity of Cys420 to readily form a sulfenic acid derivative was also shown by first reducing aerobically purified wild-type CrtJ with DTT, followed by removal

Table 2. Oxidative modifications of CrtJ observed through LC-ESI-MS/MS.

Residue	Sequence	Cys	Modification	Calculated mass (Da)[a]	Charge state	Observed *m/z*[b]	Treatments: DTT	DTT → H_2O_2	DTT → air
9–32	VSPDLLADIVTSACDIALVVSPGR	C22	–SH	2410.3	3+	804.2	+[c]	+	+
246–250	LLLCR	C249	–SH	616.4	2+	309.2	+	+	+
419–432	MC*IETALELTGNNR	C420	–SH	1563.7	2+	782.8	+	+	+
			–S-DAz-2	1756.8	2+	879.4	–[d]	+	+
246–250	LLLCR	C249	–S-S–	2178.1	3+	727.1	–	+	+
419–432	MCIETALELTGNNR	C420							

a. Calculated mass of the tryptic peptides containing cysteine modifications.
b. Extracted ion chromatogram (EIC) and collision-induced dissociation (CID) spectra of all observed peptides together with the de novo sequencing fragment ion assignments for the peptides CID spectra are shown in Figs S2–S6.
c. The plus sign indicated the peptide has been observed in the sample with specific treatment.
d. The minus sign indicated the peptide has not been observed in the sample with specific treatment.

of DTT. As shown in Fig. 3B, chemically reduced CrtJ cannot be labelled with DAz-2 indicating that all of the Cys are in a free thiol state. Subsequent oxidation of reduced CrtJ by incubating CrtJ with 1 equiv of H_2O_2 for 30 min or re-exposing to air for 30 min at room temperature can be readily labelled by DAz-2 (Fig. 3B). This indicates that Cys420 can be readily converted to sulfenic acid upon exposure to H_2O_2 and O_2.

In vivo analysis of Cys420 was undertaken by constructing chromosomally encoded ectopically FLAG tagged derivatives of CrtJ that either contained wild type or C420A mutated CrtJ sequences. These strains were grown either aerobically or anaerobically (photosynthetically) and then exposed to DAz-2 that is capable of freely diffusing through the membrane and reacting with the sulfenic acid oxidized derivative of cysteine. After treatment of cells with DAz-2, CrtJ–FLAG was isolated from cell lysate by anti-FLAG affinity gel purification and reacted with phosphine-biotin via Staudinger ligation. Labelled proteins were then separated by SDS-PAGE and detected using streptavidin-HRP via Western blotting. In parallel, the presence of the FLAG epitope was determined by Western blot analysis using anti-FLAG M2-HRP. The results of the *in vivo* labelling experiments shows that wild-type CrtJ–FLAG can be labelled by DAz-2 in aerobically grown cells but not in photosynthetically grown cells (Fig. 3C). We also observed that a strain that contains a CrtJ–FLAG derivative with a C420A mutation does not exhibit labelling with DAz-2 under aerobic growth condition (Fig. 3D). These results clearly indicate that exposure of *R. capsulatus* cells to oxygen results in the formation of a sulfenic acid derivative of CrtJ at Cys420 *in vivo*.

Mass spectrometric identification of Cys oxidation derivatives

We addressed what types of redox modifications may be occurring at specific Cys by undertaking liquid chromatography electrospray tandem ionization mass spectrometric analysis (LC-ESI-MS/MS). We first treated reduced CrtJ with hydrogen peroxide or air and then with DAz-2 that covalently reacts with sulfenic acid (Leonard *et al.*, 2009), in order to stabilize (trap) the sulfenic acid group prior to trypsin digestion and LC-ESI-MS/MS analysis. All Cys-containing peptides that were observed by mass spectrometry (MS), and verified by tandem mass spectrometry (MS/MS) analysis, are shown in Table 2. Figures S2–S6 also contain the extracted ion chromatograms (EICs) and collision-induced dissociation (CID) spectra of all observed peptides together with the de novo sequencing fragment ion assignments for the peptides CID spectra (Hunt *et al.*, 1986).

Air purified CrtJ that was reduced with 10 mM DTT prior to tryptic digestion yielded three clearly identified peptides that contained cysteines in a reduced state as free thiols (–SH). Specifically, we observed an $[M+3H]^{+3}$ ion at *m/z* 804.2 corresponding to the tryptic peptide containing Cys22 and two $[M+2H]^{+2}$ ions at *m/z* 309.2 and 782.2 corresponding to tryptic peptides containing Cys249 and Cys420 respectively (Figs S2–S4 and Table 1).

We similarly used LC-ESI-MS/MS to analyse air oxidized and hydrogen peroxide exposed CrtJ. Under these oxidizing conditions a peptide containing Cys22 was only observed in its free thiol form, while peaks corresponding to oxidized derivatives of tryptic peptides containing Cys249 and Cys420 were observed. Specifically, a peak at *m/z* 879.4 corresponding to a $[M+2H]^{+2}$ tryptic peptide containing DAz-2 labelled Cys420 was observed in both air and H_2O_2 treated samples. This indicates that Cys420 is indeed oxidized to a sulfenic acid derivative, which confirms the Western blot results, above (Fig. S5). In addition, a peak at *m/z* 727.1 corresponding to a $[M+3H]^{+3}$ cross-linked tryptic peptide containing a disulfide bridge between Cys249 and Cys420 was also observed in both air and H_2O_2 treated samples (Fig. S6). A sulfonic acid derivative ($–SO_3H$) of Cys249, and sulfinic acid ($–SO_2H$)

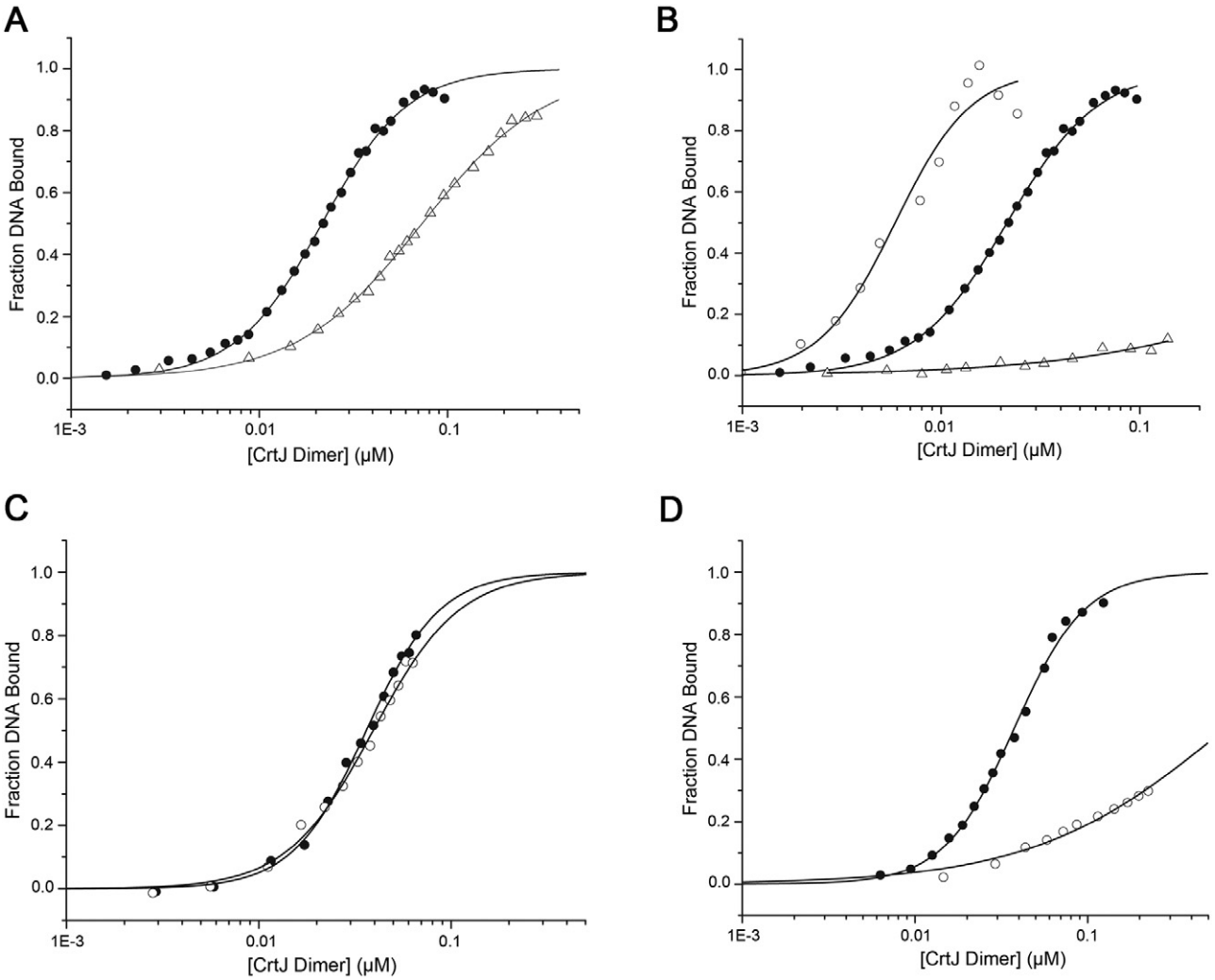

Fig. 4. Representative normalized fluorescence anisotropy-based *bchC* promoter probe DNA binding isotherms for (A) aerobic binding of WT CrtJ (solid circles), CrtJ C249A (open triangles); (B) aerobic binding of WT CrtJ (solid circles), CrtJ C420A (open triangles), C420S (open circles); (C) aerobic binding of CrtJ C420S in the presence (open circles) or absence of 5 mM DTT (solid circles); (D) aerobic binding of CrtJ C249A in the presence (open circles) or absence of 5 mM DTT (solid circles). Continuous line through each binding isotherm represents a non-linear regression analysis fit to Hill equation.

oxidized forms of both Cys249 and Cys420 were also detected but at lower intensities in both the H_2O_2 and air exposed samples. Only a small fraction of CrtJ formed these higher oxidization derivatives, which indicates that these irreversible sulfinic/sulfonic modifications may carry no physiological significance and are likely subjected to degradation *in vivo*.

Ser and Ala mutations of Cys420 differentially affect DNA binding affinity in vitro

We conducted *in vitro* DNA binding studies using fluorescence anisotropy to the 54 bp *bchC* promoter probe using purified wild-type and mutant CrtJ. Under air oxidizing conditions, CrtJ C249A exhibited similar DNA binding affinity with $EC_{50} = 45 \pm 25$ nM, as compared with that of oxidized wild-type CrtJ that exhibits an EC_{50} 43 $\pm$ 20 nM (Fig. 4A and Table 1).

The minor DNA binding effect exhibited by the Cys249 mutation is in stark contrast to the effect of mutations at Cys420. Specifically, under air oxidizing conditions, CrtJ C420A exhibited a much lower binding affinity ($EC_{50} = 2498 \pm 1176$ nM) than did air oxidized wild-type CrtJ ($EC_{50} = 43 \pm 20$ nM). Interestingly, a C420S mutation, that presumably mimics a sulfenic acid derivative of cysteine, actually exhibits tighter binding to the probe ($EC_{50} = 11 \pm 7$ nM) than does air oxidized wild-type CrtJ ($EC_{50} = 43 \pm 20$ nM) (Fig. 4B and Table 1). The C420S mutation is also constitutively active as it no longer exhibits changes in DNA binding affinity in response to an alteration

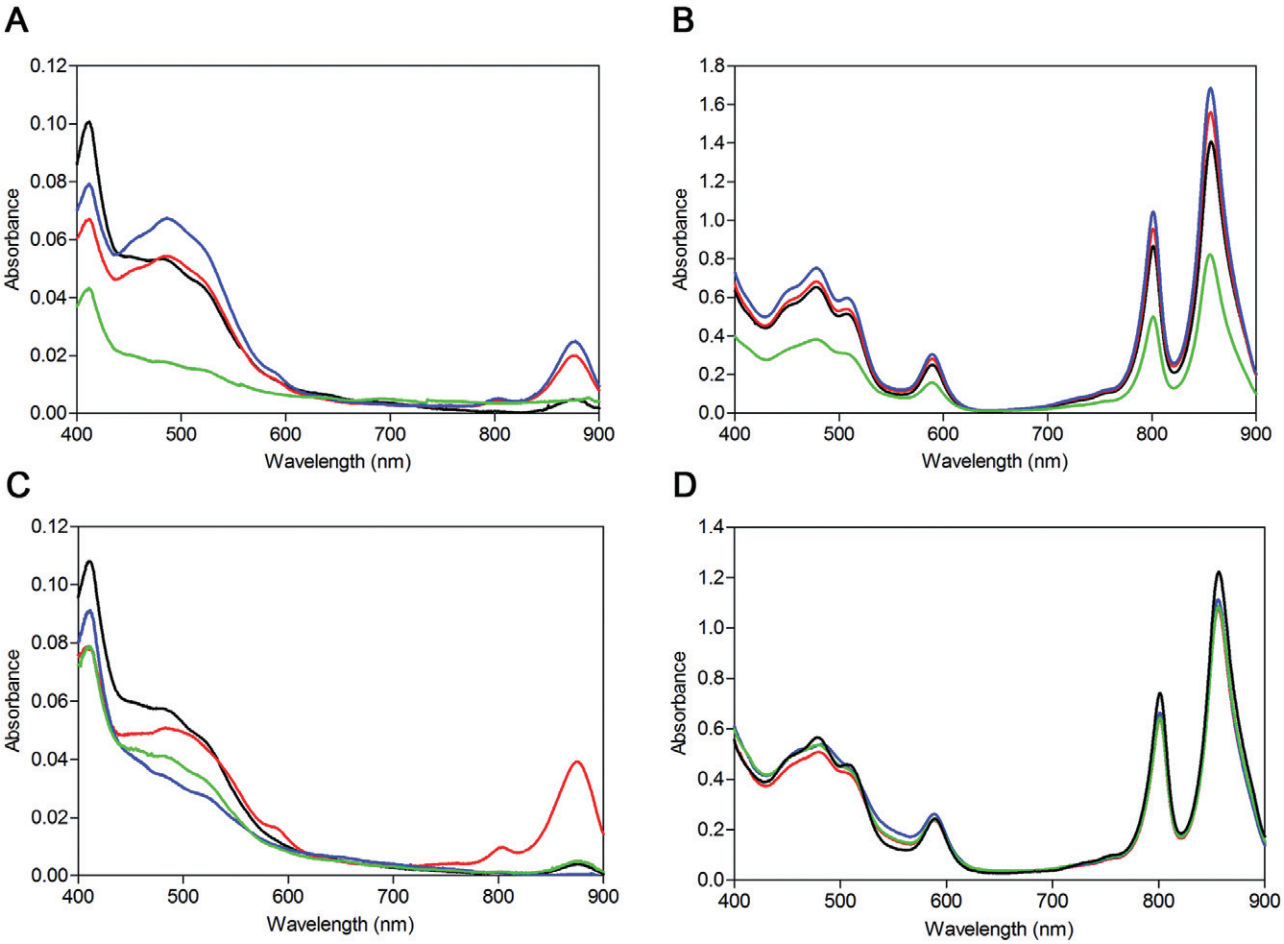

Fig. 5. Spectral scans of photopigments in *R. capsulatus* carrying CrtJ Cys420 and Cys249 mutants.
A. Spectral scans of crude cell extracts from aerobically grown wild-type SB1003 cells (black line), *crtJ* deletion CD2-4 (red line), *crtJ* C420A mutant (blue line) and *crtJ* C420S mutant (green line) cells.
B. Spectral scans of crude cell extracts from photosynthetically grown cells as described in (A).
C. Spectral scans of crude cell extracts from aerobically grown wild-type SB1003 cells (black line), *crtJ* deletion CD2-4 (red line), *crtJ* C249A mutant (blue line) and *crtJ* C249S mutant (green line) cells.
D. Spectral scans of crude cell extracts from photosynthetically grown cells as described in (C).

in redox with an $EC_{50} = 11 \pm 7$ nM under air oxidizing conditions and an $EC_{50} = 14 \pm 7$ nM under 5 mM DTT reducing conditions (Fig. 4C). Interestingly, the DNA binding affinity of C249A mutation is still redox dependent *in vitro* as reduced CrtJ C249A has a lower binding affinity ($EC_{50} = 552 \pm 115$ nM) than does oxidized CrtJ C249A ($EC_{50} = 45 \pm 25$ nM) (Fig. 4D). These observations suggest that the redox dependent DNA binding activity exhibited by CrtJ is highly dependent on altering the oxidation state of Cys420.

Mutations of Cys420 result in distinct phenotypes in vivo

A chromosomally encoded C420S point mutation in *crtJ* resulted in colonies that appear paler, while a *crtJ* C420A mutation resulted in colonies that appeared darker, than those derived from wild-type parent cells (SB1003). Spectral analysis of aerobically and anaerobically (photosynthetically) grown cultures demonstrate that the C420A mutant shows elevated aerobic pigment levels that are similar to that observed with the *crtJ* deletion strain CD2-4 (Fig. 5A and B). This is consistent with the *in vitro* DNA binding assays (Fig. 4B), which indicates that this mutation significantly impairs the DNA binding activity of CrtJ. Similar analysis of the C420S mutant showed that this strain exhibits significantly reduced photopigment synthesis as compared with the wild-type parent under both aerobic and anaerobic conditions (Fig. 5A and B), which is also consistent with *in vitro* DNA binding assays (Fig. 4B and C). In contrast to Cys420 mutant strains, Ala and Ser mutant strains at Cys249 showed similar photopigment levels as compared with the wild-type parent strain (Fig. 5C and D). This further underscores that redox modification of Cys420 has a more significant effect on con-

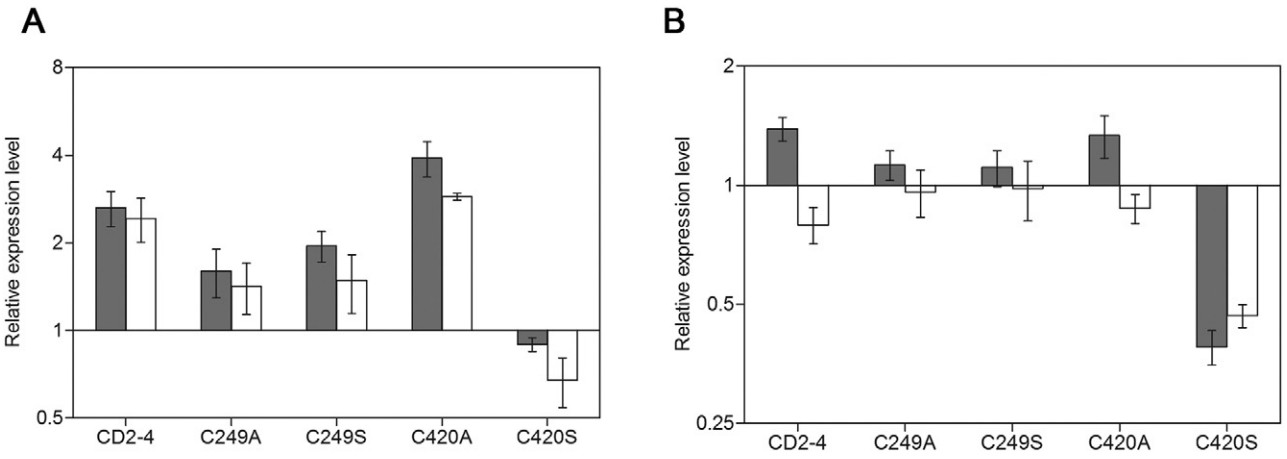

Fig. 6. Quantitative reverse transcriptase (QRT)-PCR showing the relative expression level of *bchC* (grey bar), *pucB* (white bar) in the *crtJ* deletion strain CD2-4, the *crtJ* C249A, *crtJ* C249S, *crtJ* C420A and *crtJ* C420S mutant strains as compared with wild-type SB1003 cells (define its transcription amount as 1).
A. Expression levels of mutant strains relative to wild-type cells under aerobic growth condition.
B. Expression levels of mutant strains relative to wild-type cells under anaerobic (photosynthetic) growth condition.
Error bars represent standard error of the mean ($n = 3$).

trolling the activity of CrtJ than does redox modification of Cys249.

We also used quantitative real-time PCR (polymerase chain reaction) to assay expression of the *bchC* and *puc* photosystem genes that are repressed by CrtJ. As shown in Fig. 6A, under aerobic condition, the *crtJ* C420A mutant exhibited elevated *bchC* and *pucB* expression to a level (2.5- to 4-fold as compared with wild-type parent strain) that was similar to the *crtJ* deletion strain CD2-4. The 2- to 4-fold elevation exhibited by the null mutation of CrtJ is consistent to what has been reported in previous studies (Ponnampalam *et al*., 1995; Masuda *et al*., 2002). In contrast, the C420S mutant exhibited increased repression of *bchC* and *pucB* expression as compared with the parent under aerobic conditions (Fig. 6A). The effect of the C420S mutant is also consistent with *in vitro* DNA binding assays which show that the Cys to Ser mutation leads to increased DNA binding activity over that observed with oxidized wild-type CrtJ (Fig. 4B). In contrast to Cys420 mutant strains, C249A and C249S mutants both elevated aerobic expression level of *bchC* and *pucB* compared with wild-type parent strain, but not to the same extend as does the C420A mutant. As shown in Fig. 6B, under anaerobic (photosynthetic) condition, the *crtJ* deletion strain CD2-4 and the *crtJ* C249A, C249S, C420A mutant showed similar *bchC* and *pucB* expression level compared with wild-type parent strain. In contrast, the C420S mutant exhibited decreased *bchC* and *pucB* expression as compared with the parent under anaerobic condition (Fig. 6B). This is also consistent with *in vitro* DNA binding assays which show that C420S mutant protein binds DNA with high affinity under anaerobic condition (Fig. 4C). Quantitative real-time PCR results showed that mutation on CrtJ Cys420 has more severe effect on the photosystem gene expression than on CrtJ Cys249, under both aerobic and anaerobic conditions.

Discussion

Prior studies from our laboratory demonstrated that DNA binding by CrtJ was redox regulated (Ponnampalam and Bauer, 1997). Given that CrtJ does not contain any cofactors such as metals or flavin (Ponnampalam and Bauer, 1997), and that an Ala mutation at Cys420 disrupted DNA binding, the involvement of a redox active cysteine was implicated (Ponnampalam and Bauer, 1997; Masuda *et al*., 2002). A model from these studies proposed that DNA binding was stimulated by the oxidative formation of an intramolecular disulfide bond between cysteine residues Cys249 and Cys420 (Zheng *et al*., 1998; Masuda *et al*., 2002). However, the results presented in our current study show that redox regulation of CrtJ activity involves a more complex event than simple disulfide bond formation. Specifically, we observed that an Ala substitution mutation of Cys420 has a much stronger *in vivo* phenotype than does an Ala substitution at Cys249 (Fig. 5). This disparity would not be the case if disulfide bond formation is the only contributor to the stimulation of DNA binding activity. In addition, an alignment of CrtJ homologues from different species shows that only Cys420 is conserved among known redox responding homologues (Fig. S1). Interestingly, *Bradyrhizobium sp*. ORS278 actually has two CrtJ homologues, PpsR1 that responds to redox potential and PpsR2 that responds to light intensity through a repressor (PpsR2)-antirepressor (phytochrome) interaction (Jaubert *et al*., 2004). In this species, redox responding PpsR1 only

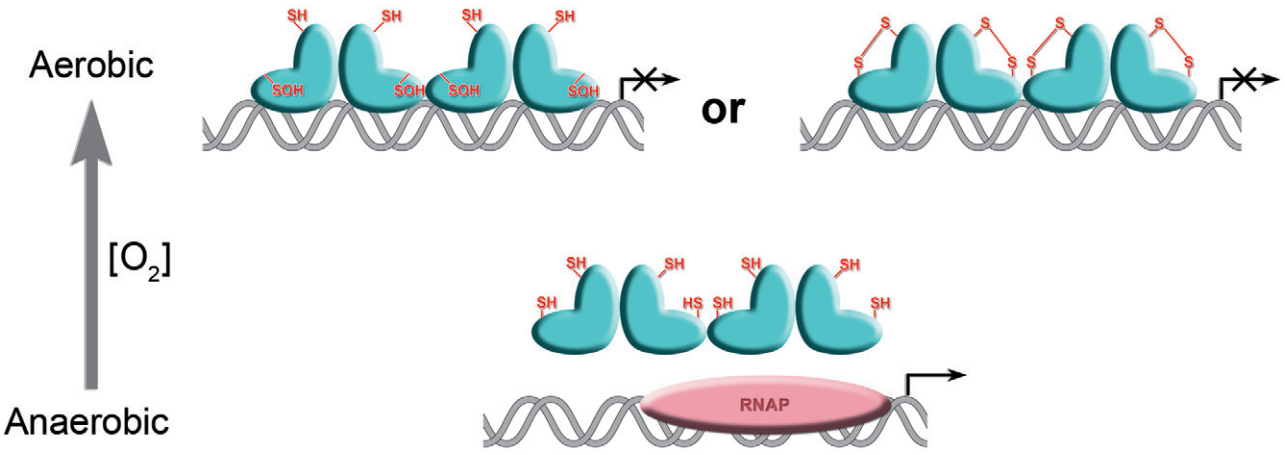

Fig. 7. Model for CrtJ redox regulation. Under anaerobic growth condition (bottom) Cys249 and Cys420 of CrtJ are in the free thiol form impeding the ability of CrtJ to bind DNA. RNA polymerase binds DNA and subsequently induces photosystem gene expression. Under aerobic condition (top), oxygen promotes the mixed formation of sulfenic acid at Cys420 or a disulfide bond between Cys249 and Cys420. These two forms of oxidized CrtJ both bind DNA tightly and repress photosystem gene expression.

has Cys420 present and not Cys249 while the light responding PpsR2 that does not contain any cysteine residues, is also no longer redox responsive (Jaubert *et al*., 2004). These results indicated that the DNA binding activity of CrtJ is likely regulated by the redox state of Cys420 which does not always lead to disulfide bond formation.

When initiating this study, we modified our model to include the possible role of additional oxidative derivatives of cysteine beyond disulfide bond formation based on the results of Stamler and colleagues (Kim *et al*., 2002) who showed that redox regulation of OxyR involved the formation of a variety of different cysteine oxidative modifications. Specifically, they showed that –SH, –SOH, –SSG, or –SNO derivatives of Cys199 resulted in unique conformational changes of OxyR that differentially regulated DNA binding activity (Kim *et al*., 2002). Our data suggest that Cys420 in CrtJ also undergoes a variety of oxidative modifications upon exposure to air leading to the formation of –S-S–, –SOH, $–SO_2H$, $–SO_3H$ derivatives. Based on quantification of free thiols in purified CrtJ, and its reactivity with sodium arsenite, we can estimate that ~ 70% of Cys420 in air exposed CrtJ forms a sulfenic acid (–SOH) modification and ~ 20% of Cys420 forms disulfide bond. There is also a small portion (~ 0.2 per monomer) of cysteine residues in CrtJ forming higher irreversible oxidative derivatives such as sulfinic acid ($–SO_2H$) or sulfonic acid ($–SO_3H$) (Fig. 2A). We suspect that these minor sulfinic or sulfonic acid adducts are either artefacts of purification, or if they occur *in vivo*, are destined to degradation as appears to be case for OhrR (Soonsanga *et al*., 2008). This is contrasted by oxidation of Cys420 either to –SOH or to a disulfide with Cys249 that seem to stimulate DNA binding activity (Fig. 7).

The LC-ESI-MS/MS analysis also indicated that exposure of CrtJ to air or to H_2O_2 leads to disulfide bond and sulfenic acid formation. Disulfide bond formation does affect the DNA binding activity of CrtJ as observed by the different effects of DTT (~ 20-fold) and sodium arsenite (~ 2-fold) on the *in vitro* DNA binding activity of CrtJ (Fig. 2C and Table 1). However, we suspect that the amount of disulfide bond formation *in vivo* is relatively low since air oxidation of CrtJ *in vitro* results in ~ 70% of Cys420 in CrtJ that contain a sulfenic acid modification. Oxidation of cysteine to sulfenic acid (–SOH) is emerging as an important post-translational modification that regulates protein function in response to oxidative stress (Saurin *et al*., 2004; Charles *et al*., 2007; Reddie and Carroll, 2008; Leonard *et al*., 2009). A recent proteomic study using the cell permeable, sulfenic acid (–SOH)-specific probe DAz-2 has identified 14 known and 175 new proteins that are capable of forming sulfenic acid in HeLa cells (Leonard *et al*., 2009). These identified proteins are involved in signal transduction, DNA repair, metabolism, protein synthesis, redox homeostasis, nuclear transport, vesicle trafficking, and ER quality control (Leonard *et al*., 2009). Individual studies also revealed that sulfenic acid can act as an oxidative stress sensor to regulate enzyme activity such as cysteine protease papain (Lin *et al*., 1975) and protein tyrosine phosphatases (Denu and Tanner, 1998), function as an antioxidant such as human serum albumin (Carballal *et al*., 2003), and modulate activity of transcriptional factors such as Gpx3/Yap1 in *Saccharomyces cerevisiae* (Paulsen and Carroll, 2009), OhrR in *Bacillus subtilis* (Fuangthong and Helmann, 2002), OxyR in *E. coli* (Kim *et al*., 2002). Most SOH-forming transcriptional factors are responding to reactive oxygen species (ROS) such as H_2O_2; however, our results demonstrate that the sulfenic acid (–SOH) modification on CrtJ Cys420 is also response to the availability of oxygen. To our knowledge, this is the first example that a transcriptional factor uses

–SOH as a sensor for environmental oxygen. This is reasonable considering that oxygen rather than H_2O_2 is the physiologically relevant signal for the regulation of bacteriochlorophyll genes that are regulated by CrtJ (Ponnampalam *et al*., 1995). When bacteriochlorophyll is light excited in the presence of oxygen, it is capable of generating singlet oxygen as a by-product of photosynthesis. Since singlet oxygen is toxic to the cells, these cells utilize CrtJ to aerobically repress the synthesis of bacteriochlorophyll.

The redox active Cys420 in CrtJ is located in the first helix of the HTH-motif (Fig. S1). To our knowledge this is the only reported case where a redox active Cys is actually located in a DNA binding domain in prokaryotes. The changes of oxidative states on this Cys may promote a conformational change in the HTH-motif, resulting in different DNA binding activity. This is distinctly different from OxyR and the MarR family members OhrR (Hong *et al*., 2005) in *B. subtilis* and SarZ in *Staphylococcus aureus* (Poor *et al*., 2009), in which a redox active cysteine is located away from the DNA binding domain. In the case of SarZ, a redox active Cys at N-terminus hydrophobic pocket is capable of forming sulfenic, sulfinic and sulfonic acid derivatives with the sulfinic and sulfonic acid modifications thought to cause a large global conformational change in the protein leading to an alteration of the DNA binding domain (Poor *et al*., 2009). Structural studies on the reduced or oxidized derivative of CrtJ co-complex with DNA will also be needed to determine details of how alterations of Cys420 lead to alteration of the DNA binding activity of CrtJ.

Experimental procedures

Plasmid and strain construction

The expression plasmid pSUMO::CrtJ was constructed by subcloning from pET28::CrtJ (Ponnampalam and Bauer, 1997) plasmid into a modified pSUMO vector (LifeSensors), using NdeI and HindIII restriction sites. Cys mutations in the pSUMO-CrtJ construct were constructed by QuickChange. *crtJ* deletion strain CD2-4 and *crtJ* mutant strains C249A, C249S, C420A, C420S were generated as previously described (Masuda *et al*., 2002). CrtJ–FLAG and CrtJ C420A–FLAG expressing strains were constructed by fusing 7 amino-acid long FLAG epitope into the C-terminus of CrtJ followed by a stop codon in the suicide plasmid pZJD3. FLAG fusions were integrated into SB1003 chromosome as described previously (Dong *et al*., 2002).

Overexpression and purification of CrtJ and CrtJ mutants

The pSUMO::CrtJ plasmid was transformed into *E. coli* strain BL21 (DE3) and the recombinant protein SUMO-CrtJ was aerobically overexpressed by induction of a 1 l culture with 1 mM IPTG at 16°C overnight (12–16 h). Cells were harvested and resuspended in 40 ml nickel column loading buffer composed of 20 mM Tris-HCl (pH 8.0), 150 mM NaCl, 5 mM imidazole and 10% glycerol and lysed by passing through a French pressure cell three times at 18 000 psi. The lysate was clarified by centrifugation at 30 000 *g* for 30 min at 4°C. The resultant supernatant was passed through a 45 μM membrane filter (Millipore) and loaded onto a 1 ml HisTrap column (GE) with an ÄKTA chromatography system (GE), washed with 30-column volume of wash buffer containing 20 mM Tris-HCl (pH 8.0), 150 mM NaCl, 20 mM imidazole, and 10% glycerol. SUMO-CrtJ was eluted with a gradient of 20 mM imidazole to 500 mM imidazole in the loading buffer over a 15-column volume total. The SUMO tag was then proteolytically cleaved by Ulp1 protease and tag-less CrtJ was isolated by Superose 12 (S-12) size exclusion chromatography in a CrtJ standard buffer containing 20 mM Tris-HCl (pH 8.0), 500 mM NaCl, and 6% glycerol at a rate of 1 ml min^{-1}. Peak fractions were analysed by SDS-PAGE with CrtJ containing fractions collected and pooled. Typical protein yield was approximate 5 mg l^{-1} cells with protein greater than 99% pure as based on SDS-PAGE. The aerobically purified protein was stored in an anaerobic jar filled with argon gas at 4°C as CrtJ is unstable when stored for extended periods in the presence of oxygen.

Determination of protein and DNA concentration

The protein concentration was determined using the Bradford assay (Advanced Protein Assay Reagent, Cytoskeleton) with BSA as a standard. DNA oligomer absorbance at 260 nm was measured and DNA concentration was determined using the extinction coefficient at 260 nm. Each sample was measured three times and the average concentration was obtained.

Fluorescence anisotropy-based DNA binding experiments

A 5′-fluorescein labelled, 54 bp oligomer of the *bchC* promoter probe was hybridized to its unlabelled complementary strand at a labelled to unlabelled ratio of 1.0:1.1 by heating to 95°C for 10 min followed by slow-cooling to room temperature. Fluorescence anisotropy experiments used an ISS PC1 spectrofluorometer fitted with polarizers in the L format. Purified CrtJ sample (~ 10 μM) was titrated into 10 nM duplex in the basic CrtJ-DNA binding buffer (50 mM Tris-HCl at pH 8.0, 300 mM NaCl, 2 mM $MgCl_2$, and 6% glycerol) at 25°C. Anisotropy was monitored by exciting the fluorescein at 476 nm with the average of five measurements recorded for each addition. Additives such as DTT, sodium arsenite, or H_2O_2 were added to the basic binding buffer prior to addition of CrtJ. Reduction of CrtJ was obtained by incubation with 100 mM DTT for 1 h at room temperature in an anaerobic hood followed by repeated concentration and redilution into CrtJ standard buffer for a total five times in a 30K Amicon Ultra Centrifugal Filter. The resulting data were fitted to a cooperative binding model, using Hill equation (Eq. 1) with OriginPro 8.5. Parameters of the fit included anisotropies of free and bound DNA (A_D and A_{DP}). Hill coefficient (n) and the apparent dissociation constants (K_{app}) were both obtained.

$$\log\frac{A-A_D}{A_{DP}-A} = n\cdot\log[P_2]-\log K_{app} \quad (1)$$

$K_{app} = (EC_{50})^n$; P_2: CrtJ dimer concentration. EC_{50} corresponds to the dimer concentration when DNA binding sites are half-occupied.

Free thiol quantification

Free thiols were quantified by adding aliquots of 0.2 mM *p*-CMB in 0.1 M Tris-HCl at pH 7.3 (Boyer, 1954; Turell *et al.*, 2008) to 20 μM of CrtJ with increases in absorbance at 250 nm recorded. Air oxidized CrtJ was obtained though standard purification procedure. For other treatments, CrtJ was incubated with 1 equiv of H_2O_2 for 30 min at room temperature or with 20 mM sodium arsenite for 1 h at 37°C. DTT reduction of CrtJ was the same as described in the fluorescence anisotropy experiments.

NBD-Cl assay

Reduced or oxidized CrtJ was incubated with 2 equiv of NBD-Cl in dimethylsulphoxide in an anaerobic hood for 1 h at room temperature in the dark (Birkett *et al.*, 1970). Modified CrtJ was concentrated and rediluted into CrtJ standard buffer five times with Amicon Ultra Filters (30 kD, Millipore) in an anaerobic hood to remove free NBD-Cl. Modified CrtJ was then subjected to spectral scan from 300 nm to 900 nm with a DU640 Beckman spectrophotometer (Ellis and Poole, 1997).

In vitro *DAz-2 labelling of sulfenic acid in recombinant CrtJ*

DAz-2 labelling of purified recombinant CrtJ involved a modified method described by K. Reddie *et al.* (Reddie *et al.*, 2008). Briefly, 2.0 μg of freshly prepared CrtJ was reacted with 0.25 mM DAz-2 or DMSO for 1 h at 37°C. In experiments where CrtJ was treated with H_2O_2 or air oxygen, CrtJ was first reduced as described above in the fluorescence anisotropy experiments. Reduced CrtJ was incubated with 1 equivalent H_2O_2 at RT for 30 min in the hood or exposed to air for 30 min at RT outside the hood.

Mass spectrometry

CrtJ protein (~ 10 μM) was DAz-2 labelled as described above and then digested with 20-fold (weight ratio) sequencing grade trypsin (Roche Applied Science) overnight at 37°C in 100 mM Tris-HCl (pH 8.5), 500 mM NaCl, and 6% glycerol. The resulting samples were then analysed by liquid chromatography electrospray tandem ionization mass spectrometric analysis (LC-ESI-MS/MS) with liquid chromatography (LC) performed utilizing an Agilent 1200 Series binary capillary flow pump (Agilent Technologies). Mobile phases were degassed with a vacuum degasser and the samples were injected via an autosampler (Agilent Technologies). LC separation was accomplished using a Zorbax® 300 SB-C18 column (75 × 0.3 mm, 3.5 μm particle size) from Agilent technologies. Mobile phase A consisted of 97%/3%/0.1% water/acetonitrile/formic acid, while mobile phase B was composed of 97%/3%/0.1% acetonitrile/water/formic acid. A linear gradient from 3% B to 45% B over 45 min at a flow rate of 4 μl min^{-1} with a total run time including column re-equilibration of 80 min. 8 μl of tryptic digests of CrtJ (~ 10 μM) was injected using the capillary-flow pump onto the C18 column. Separated peptides were detected and identified using an ultra-high capacity ion-trap mass spectrometer (Bruker Daltonik GmbH, Bremen, Germany). Electrospray ionization (ESI) in positive ion mode was performed with spray voltages of 4200V, nebulizer and dry gas pressures of 10 and 5 psi respectively, and a dry gas temperature of 300°C. ESI source parameters such as the voltages on the skimmer, Capillary exit, and octopole RF and DC voltages were optimized using direct infusion of 5 μmol l^{-1} Renin solution at a flow rate of 4 μl min^{-1}. Standard 'enhanced' mode was used for MS and MS/MS analyses with the *m/z* scanning range set to 300–1800 and the number of MS and MS/MS averages set to 3. The Smart Parameter Setting (SPS) and the Ion Charge Control (ICC) were set 'on' with a smart target of 150 000 and a maximum accumulation time of 200 ms. An MS scan operated in an automated MS^2 mode was followed by a CID scan of the three most intense ions detected in the MS scan that were above an absolute intensity threshold of 250 000 excluding singly charged ions. The CID fragmentation amplitude was 1V, the isolation width was 4.0 *m/z*, and the cycle was continuously repeated throughout the entire separation with the active exclusion set to 1.5 min for a repeat count of 3 spectra. Data analysis was performed using the DataAnalysis version 3.4 and the Biotools version 3.0 programs from Bruker Daltonics and each CID spectrum of interest was analysed manually using de novo peptide sequencing rules (Hunt *et al.*, 1986).

In vivo *DAz-2 labelling of CrtJ–FLAG*

Aerobic cultures of CrtJ–FLAG expressing *R. capsulatus* cells were grown at 34°C in 250 ml of PY medium in 3 l baffled flasks shaking at 300 r.p.m. to early log phase. Anaerobic cultures were grown photosynthetically in an air-tight screw-cap bottle in PY medium at 30°C until late log phase. Cells were chilled on ice, collected by centrifugation at 6000 *g* and washed three time with 50 ml cold TBS containing 50 mM Tris-HCl (pH 7.4), 150 mM NaCl. Cell pellets were resuspended in 3 ml TBS and incubated with 5 mM DAz-2 or DMSO at 4°C over night. Cells were then washed three times with 50 ml cold TBS and resuspended in 3 ml 50 mM Tris-HCl (pH 7.4), 150 mM NaCl, 1% Triton X-100, to which 1 mg ml^{-1} lysozyme and 20 μl protease inhibitor cocktail (Sigma) were added. Cell lysate was prepared by sonication. Supernatant was collected by centrifugation at 20 000 *g* for 20 min. To enrich the labelled CrtJ–FLAG, the supernatant was incubated with EZView Red ANTI-FLAG M2 affinity gel (Sigma) over night at 4°C. The resin was collected at 8200 *g* for 30 s and washed three times with 0.5 ml TBS. DAz-2 labelled CrtJ–FLAG was then eluted with 100 μl 150 ng μl^{-1} 3× FLAG peptide (Sigma).

Staudinger ligation and Western blot analysis

DAz-2 labelled recombinant CrtJ or CrtJ–FLAG was conjugated to biotin via Staudinger ligation with 0.25 mM

phosphine-biotin for 2 h at 37°C. Biotinylation reactions were terminated by the addition of 0.5 ml cold acetone and kept in –80°C for 30 min. The precipitated protein then was centrifuged at 20 000 *g* for 15 min and protein pellets was resuspended in TS buffer containing 50 mM Tris-HCl (pH 7.4) and 1% SDS.

Biotinylated proteins in TS buffer were separated by 15% SDS-PAGE and then electro-transferred to nitrocellulose membrane (Perkin-Elmer). The membrane was blocked in 3% bovine serum albumin (BSA) (Fisher) in phosphate-buffered saline Tween-20 (PBST: 1.4 mM KH_2PO_4, 8 mM Na_2HPO_4, 140 mM NaCl 2.7 mM KCl, 0.05% Tween 20, pH 7.3) overnight at 4°C or 1 h at room temperature. The membrane was then incubated with 1:50 000 strepvidin-HRP (GE Healthcare) in PBST for 1 h at room temperature, and washed three times by 50 ml PBST followed by developing with Amersham ECL prime Western blotting detection reagents (GE Healthcare). For *in vitro* analysis with isolated recombinant CrtJ proteins that were transferred to the membrane were visualized by staining with Ponceau S (Sigma) (Ponceau S dye is a sodium salt of diazo dye, which is used for rapid reversible staining of protein bands on nitrocellulose or polyvinylidene difluoride membranes). CrtJ–FLAG present in whole cells for *in vivo* analysis were identified using monoclonal ANTI-FLAG M2-HRP antibody (Sigma).

Spectral analysis on R. capsulatus wild type and mutants

Rhodobacter capsulatus wild-type and mutant strains were grown aerobically or photosynthetically to early-exponential phase in PY salts medium. 8.5 ml of cultures was chilled on ice, harvested by centrifugation at 4400 *g*, resuspended in a 1 ml buffer of 20 mM Tris-HCl (pH 8.0), 150 mM NaCl and lysed by sonication three times with a 15 s exposure. Cell lysate was clarified by centrifugation at 15 000 *g* for 10 min. Supernatants were scanned in the range of 300 nm to 900 nm on a DU640 Beckman spectrophotometer.

RNA isolation, quantitative real-time PCR (QRT-PCR)

Rhodobacter capsulatus wild-type and mutant strains were grown aerobically or anaerobically (photosynthetically) to early-exponential phase in PY salts medium. 1 ml cells were harvest with total RNA of each sample extracted using ISOLATE RNA kits (Bioline). RNA samples were then treated with TURBO DNase (Ambion) and final concentrations were measured by NanoDrop (Thermo Scientific). A typical OD_{260} to OD_{280} ratio of RNA samples were approximately 2.0.

The QRT-PCR analysis of gene expression utilized QRT-PCR Master Mix Kit (Agilent) with 10 ng of RNA sample used in a 25 µl reaction. The cDNA synthesis was at 50°C for 30 min followed by QRT-PCR. A two-step PCR reaction was used, consisting a product melt at 95°C for 30 s, followed by primer annealing and DNA polymerase elongation at 60°C for 1 min. As an internal control, the house-keeping gene *rpoZ* that encodes DNA-directed RNA polymerase omega subunit was used. All primers used in QRT-PCR are shown in Table S1.

Acknowledgements

This study is supported by Grant R37GM040941 from the National Institutes of Health awarded to C.E.B. and funding from the Camile Henry Dreyfus Teacher Scholar Award and the American Heart Association Scientist Development Award (0835419N) to K.S.C.

References

Bauer, C.E. (2001) Regulating synthesis of the purple bacterial photosystem. In *Regulation of Photosynthesis*. Aro, E., and Andersson, B. (eds). Dodrecht: Kluwer Academic Press, pp. 67–83.

Bauer, C.E., and Bird, T.H. (1996) Regulatory circuits controlling photosynthesis gene expression. *Cell* **85:** 5–8.

Birkett, D.J., Price, N.C., Radda, G.K., and Salmon, A.G. (1970) The reactivity of SH groups with a fluorogenic reagent. *FEBS Lett* **6:** 346–348.

Boyer, P.D. (1954) Spectrophotometric study of the reaction of protein sulfhydryl groups with organic mercurials. *J Am Chem Soc* **76:** 4331–4337.

Carballal, S., Radi, R., Kirk, M.C., Barnes, S., Freeman, B.A., and Alvarez, B. (2003) Sulfenic acid formation in human serum albumin by hydrogen peroxide and peroxynitrite. *Biochemistry* **42:** 9906–9914.

Charles, R.L., Schroder, E., May, G., Free, P., Gaffney, P.R., Wait, R., *et al*. (2007) Protein sulfenation as a redox sensor: proteomics studies using a novel biotinylated dimedone analogue. *Mol Cell Proteomics* **6:** 1473–1484.

Cohen-Bazire, G., Sistrom, W.R., and Stanier, R.Y. (1957) Kinetic studies of pigment synthesis by non-sulfur purple bacteria. *J Cell Physiol* **49:** 25–68.

Denu, J.M., and Tanner, K.G. (1998) Specific and reversible inactivation of protein tyrosine phosphatases by hydrogen peroxide: evidence for a sulfenic acid intermediate and implications for redox regulation. *Biochemistry* **37:** 5633–5642.

Dong, C., Elsen, S., Swem, L.R., and Bauer, C.E. (2002) AerR, a second aerobic repressor of photosynthesis gene expression in *Rhodobacter capsulatus*. *J Bacteriol* **184:** 2805–2814.

Ellis, H.R., and Poole, L.B. (1997) Novel application of 7-chloro-4-nitrobenzo-2-oxa-1,3-diazole to identify cysteine sulfenic acid in the AhpC component of alkyl hydroperoxide reductase. *Biochemistry* **36:** 15013–15018.

Elsen, S., Ponnampalam, S.N., and Bauer, C.E. (1998) CrtJ bound to distant binding sites interacts cooperatively to aerobically repress photopigment biosynthesis and light harvesting II gene expression in *Rhodobacter capsulatus*. *J Biol Chem* **273:** 30762–30769.

Fuangthong, M., and Helmann, J.D. (2002) The OhrR repressor senses organic hydroperoxides by reversible formation of a cysteine-sulfenic acid derivative. *Proc Natl Acad Sci USA* **99:** 6690–6695.

Hong, M., Fuangthong, M., Helmann, J.D., and Brennan, R.G. (2005) Structure of an OhrR-ohrA operator complex reveals the DNA binding mechanism of the MarR family. *Mol Cell* **20:** 131–141.

Hunt, D.F., Yates, J.R., 3rd, Shabanowitz, J., Winston, S., and

Hauer, C.R. (1986) Protein sequencing by tandem mass spectrometry. *Proc Natl Acad Sci USA* **83:** 6233–6237.
Imhoff, J.F., Truper, H.G., and Pfennig, N. (1984) Rearrangement of the species and genera of the phototrophic 'purple nonsulfur bacteria'. *Int J Syst Bacteriol* **34:** 340–343.
Jaubert, M., Zappa, S., Fardoux, J., Adriano, J.M., Hannibal, L., Elsen, S., *et al*. (2004) Light and redox control of photosynthesis gene expression in *Bradyrhizobium*: dual roles of two PpsR. *J Biol Chem* **279:** 44407–44416.
Kim, S.O., Merchant, K., Nudelman, R., Beyer, W.F., Jr, Keng, T., DeAngelo, J., *et al*. (2002) OxyR: a molecular code for redox-related signaling. *Cell* **109:** 383–396.
Kovacs, A.T., Rakhely, G., and Kovacs, K.L. (2005) The PpsR regulator family. *Res Microbiol* **156:** 619–625.
Kullik, I., Toledano, M.B., Tartaglia, L.A., and Storz, G. (1995) Mutational analysis of the redox-sensitive transcriptional regulator OxyR: regions important for oxidation and transcriptional activation. *J Bacteriol* **177:** 1275–1284.
Leonard, S.E., Reddie, K.G., and Carroll, K.S. (2009) Mining the thiol proteome for sulfenic acid modifications reveals new targets for oxidation in cells. *ACS Chem Biol* **4:** 783–799.
Lin, W.S., Armstrong, D.A., and Gaucher, G.M. (1975) Formation and repair of papain sulfenic acid. *Can J Biochem* **53:** 298–307.
Masuda, S., Dong, C., Swem, D., Setterdahl, A.T., Knaff, D.B., and Bauer, C.E. (2002) Repression of photosynthesis gene expression by formation of a disulfide bond in CrtJ. *Proc Natl Acad Sci USA* **99:** 7078–7083.
Paulsen, C.E., and Carroll, K.S. (2009) Chemical dissection of an essential redox switch in yeast. *Chem Biol* **16:** 217–225.
Penfold, R.J., and Pemberton, J.M. (1991) A gene from the photosynthetic gene cluster of *Rhodobacter Sphaeroides* Induces *Trans* suppression of bacteriochlorophyll and carotenoid levels in *R. Sphaeroides* and *R. Capsulatus*. *Curr Microbiol* **23:** 259–263.
Ponnampalam, S.N., and Bauer, C.E. (1997) DNA binding characteristics of CrtJ. A redox-responding repressor of bacteriochlorophyll, carotenoid, and light harvesting-II gene expression in *Rhodobacter capsulatus*. *J Biol Chem* **272:** 18391–18396.
Ponnampalam, S.N., Buggy, J.J., and Bauer, C.E. (1995) Characterization of an aerobic repressor that coordinately regulates bacteriochlorophyll, carotenoid, and light harvesting-II expression in *Rhodobacter capsulatus*. *J Bacteriol* **177:** 2990–2997.
Poor, C.B., Chen, P.R., Duguid, E., Rice, P.A., and He, C. (2009) Crystal structures of the reduced, sulfenic acid, and mixed disulfide forms of SarZ, a redox active global regulator in *Staphylococcus aureus*. *J Biol Chem* **284:** 23517–23524.
Reddie, K.G., and Carroll, K.S. (2008) Expanding the functional diversity of proteins through cysteine oxidation. *Curr Opin Chem Biol* **12:** 746–754.
Reddie, K.G., Seo, Y.H., Muse Iii, W.B., Leonard, S.E., and Carroll, K.S. (2008) A chemical approach for detecting sulfenic acid-modified proteins in living cells. *Mol Biosyst* **4:** 521–531.
Saurin, A.T., Neubert, H., Brennan, J.P., and Eaton, P. (2004) Widespread sulfenic acid formation in tissues in response to hydrogen peroxide. *Proc Natl Acad Sci USA* **101:** 17982–17987.
Soonsanga, S., Lee, J.W., and Helmann, J.D. (2008) Oxidant-dependent switching between reversible and sacrificial oxidation pathways for *Bacillus subtilis* OhrR. *Mol Microbiol* **68:** 978–986.
Torchinsky, Y.M. (1981) Properties of SH groups. Sulfhydryl reagents. In *Sulfur in Proteins*. Torchinsky, Y.M. (ed.). Oxford: Pergamon, p. 53.
Turell, L., Botti, H., Carballal, S., Ferrer-Sueta, G., Souza, J.M., Duran, R., *et al*. (2008) Reactivity of sulfenic acid in human serum albumin. *Biochemistry* **47:** 358–367.
Zheng, M., Aslund, F., and Storz, G. (1998) Activation of the OxyR transcription factor by reversible disulfide bond formation. *Science* **279:** 1718–1721.

Supporting information

Additional supporting information may be found in the online version of this article.

Please note: Wiley-Blackwell are not responsible for the content or functionality of any supporting materials supplied by the authors. Any queries (other than missing material) should be directed to the corresponding author for the article.